Appl. Phys. B 74, 665–670 (2002)
DOI: 10.1007/s003400200834
Applied Physics B
Lasers and Optics

W. CHEIKH-ROUHOU[1,✉]
L.C. SAMPAIO[2,4]
B. BARTENLIAN[1]
P. BEAUVILLAIN[1]
A. BRUN[3]
J. FERRÉ[2]
P. GEORGES[3]
J.-P. JAMET[2]
V. MATHET[1]
A. STUPAKEWICZ[5]

Anisotropy of the optical and magneto-optical response of Au/Co/Au/Cu multilayers grown on vicinal Si (111) surfaces

[1] Institut d'Electronique Fondamentale UMR CNRS 8622, Université Paris-Sud, 91405 Orsay, France
[2] Laboratoire de Physique des Solides UMR CNRS 8502, Université Paris-Sud, 91405 Orsay, France
[3] Laboratoire Charles Fabry, UMR CNRS 8501, Université Paris-Sud, 91405 Orsay, France
[4] Centro Brasileiro de Pesquisas Físicas, Rio de Janeiro, Brazil
[5] Laboratory of Magnetism, Institute of Physics, University of Bialystok, Poland

Received: 16 October 2001
Published online: 29 May 2002 •

ABSTRACT The optical and magneto-optical second harmonic reflectivity response of Au/Co/Au/Cu multilayers grown on vicinal Si (111) substrates has been studied. These azimuthal optical non-linear experiments check the uniaxial character of the crystallinity of the Au buffer layer and the magnetic behavior of the ultrathin Co films in the metallic multilayer. They clearly show the strong dependence of the growth parameters and the misorientation of the vicinal surface on the SHG reflectivity signals. This uniaxial behavior is also correlated to linear MOKE experiments on the magnetic anisotropy with an easy magnetization axis parallel to the step edges.

PACS 01.30.Cc; 42.65.Ky; 68.37.Ef; 75.70.Cn

1 Introduction

Interface-induced magnetic properties are an important characteristic of ultrathin magnetic films. The magnetic moments at the surface can be enhanced in comparison with the bulk values, due to the change in the electronic structure associated with the reduced symmetry and the modified interatomic interactions. In addition, the presence of strain or roughness at interfaces can affect the magnetic anisotropy via magnetoelastic interactions [1]. Furthermore, the magnetic properties of ferromagnetic thin films grown on surfaces with reduced symmetry are of great technological importance and of fundamental scientific interest.

Several research groups have shown that the specific symmetry of a ferromagnetic film epitaxially grown on a vicinal substrate surface, i.e. a quasiperiodic sequence of atomic steps, will usually induce a uniaxial magnetic anisotropy. This has been found, for example, in Fe/W (001) [2, 3], Co/Cu (110) [4] and Fe/Ag (001) [5]. In these studies, single crystals miscut at a small angle against a low index surface were used as substrates. Since second harmonic generation (SHG) is sensitive to the symmetry of the surface and buried interfaces [6], it is a powerful technique to study the influence of growth parameters on the interface magnetic anisotropy and to illustrate the lowering of the symmetry induced by the step rearrangement of a vicinal substrate surface.

2 Experimental techniques

The substrates used in this study are Si (111) wafers, nominal, cut 2° and 6° off the [111] axis toward the high symmetry $[\bar{1}\bar{1}2]$ direction. This direction of misorientation allows a step mixture formation of one and three atomic heights [7, 8]; whereas the opposite direction, i.e. $[11\bar{2}]$ creates a substantial density of steps, which tend to form bunches, thus giving a rougher surface [9]. The substrates were chemically treated in order to obtain an ideally hydrogen-terminated Si (111)-(1×1) non-reconstructed surface, known to be highly stable, unreconstructed, very flat and nearly defect-free [10]. These characteristics make this system especially suitable for molecular beam epitaxy (MBE) and have favored its use as a substrate with adsorbates of very different nature. Substrate thermal heating and film growth were carried out in an MBE chamber with a base pressure below 2×10^{-10} mbar. Upon annealing in the UHV chamber up to 600 °C, the periodicity of the H−Si surface changes to form a stable 7×7 reconstruction checked by reflective high-energy electron diffraction (RHEED). The Cu ultrathin buffer layer was deposited under two different conditions: 2 monolayers (ML) at 100 °C and 4 ML at 200 °C. In order to check the dependence of the magnetic properties of Au/Co/Au on the Au buffer and Co thicknesses, we have grown different thicknesses of an Au buffer (3, 5, 10, 15 and 20 ML) and a Co film (2.5 to 15 ML) on the same substrate using a manual shutter. Finally, a 15 ML Au coverage was deposited to protect the Co layer. At the different stages of growth, a topographic study of the samples was performed using an in situ scanning tunneling microscope (STM). In order to correlate the surface morphology with the magnetic properties of the ultrathin multilayers, we have carried out polar and longitudinal magneto-optical Kerr effect (MOKE) measurements as well as second harmonic generation (SHG) experiments, checking the dependence of the results on the substrate misorientation angle, Cu growth condition and Au and Co layer thicknesses. The use of MOKE to study magnetization reversal processes has several advantages over conventional magnetometry since the

✉ Fax: +33-1/6915-4000,
E-mail: Wissem.Cheikh-Rouhou@ief.u-psud.fr

magnetization is only monitored in the region illuminated by the focused laser spot. The magnetic properties can be investigated as a function of layer thickness in one single sample, the results thus being free of the problems associated with growth parameter variations in samples grown at different times.

Compared with experiments using the linear Kerr effect, SHG experiments have the advantage of being highly surface-sensitive, capable of remote sensing and in situ measurements and applicable to any interface accessible with light. It can also be used to probe surface magnetization; in fact the non-linear optical susceptibility tensor possesses a group of non-vanishing elements induced by the presence of a finite magnetization.

The SHG measurements were performed using a femtosecond Ti:sapphire oscillator operating at $\lambda = 800$ nm and a repetition rate of 80 MHz. The laser beam was focused with a spot of 30 μm in diameter on the metallic multilayer. Its average power was about 20 mW in order to avoid damage of the sample. Taking into account the low quantum efficiency of the second harmonic generation in metallic interfaces, the doubled signal was measured using a liquid-nitrogen-cooled CCD camera after a very efficient filtering to reject the fundamental light. In order to achieve azimuthal measurements of the SHG (A-SHG) reflectivity, a special sample holder was designed to allow the azimuthal experiment to be performed exactly on the same point of the sample. These A-SHG reflectivity measurements were done systematically in the four polarization configurations: $S_{in}-S_{out}$, $S_{in}-P_{out}$, $P_{in}-P_{out}$, $P_{in}-S_{out}$, varying the azimuthal in-plane rotation angle of the sample from 0 to 360° by 5° steps around the surface normal (z-axis). The $x-y$-coordinates define the surface plane, the y-direction coinciding with the direction s of polarization, and the p-polarization corresponding to the plane of incidence, the $x-z$-plane.

3 Results and discussion

Copper deposition on Si (111)-(7 × 7) substrates leads to three-dimensional growth characterized by the appearance of small islands all over the surface for the two deposition temperatures. These islands present an anisotropic shape with a typical 10 nm lateral dimension and are locally arranged along the symmetry directions of the Si substrate (along the step edges or along directions at 60°). Thus, the duplication of the vicinal character of the Si substrate on the Cu layer cannot be directly observed using in situ STM. The current STM image, as shown in Fig. 1 for Au/Cu, allows to define the shape of the islands on the surface more precisely than the topographic one.

For Cu growth at 200 °C, the crystallinity seems to be better and the surface flatter. As shown below, this morphological difference between the two copper buffer layers strongly affects the magnetic properties of the Au/Co/Au/Cu multilayers deposited on vicinal Si (111) substrates.

Hysteresis loops were measured using polar and longitudinal Kerr effect experiments exploring all the growth parameters (various misorientations of the Si substrate, Cu deposition temperature, thicknesses of Au buffer and Co films (t_{Au} and t_{Co}, respectively)). The saturated polar Kerr rotation θ_K measured on all the samples follows the phenomenological law $\theta_K = K(t_{Co} - t^0_{Co})$, where t^0_{Co} depends on the Au/Co interface and K is a constant which depends on Au and Cu thicknesses [11]. Numerical simulations carried out under the optical multilayer approximation, which involves abrupt interfaces and makes use of optical and magneto-optical indices of the different materials constituting the magnetic multilayer, give an excellent quantitative description of the θ_K dependence on the Co thickness. Experimental results obtained on different multilayers deposited on 4 ML Cu grown at 200 °C are shown in Fig. 2, as well as magneto-optical Kerr rotation simulations where the interface contribution t^0_{Co} is the only close-fitting parameter. The reproducibility of the experimental results for all samples clearly shows that substrate misorientation has no influence on the magneto-optical polar Kerr rotation. The interface contribution t^0_{Co} is found to be 0.8 ML for thick buffer Au layers (10, 15 ML), the same as obtained on Au/Co/Au deposited on float glass. This contribution mainly arises from the band structure of the cobalt and gold atoms at the interface [12]. The value of t^0_{Co} increases as t_{Au} decreases (1.2 ML for $t_{Au} =$ 5 ML and 1.6 ML for $t_{Au} = 3$ ML). This behavior can be explained by interface roughness or $CoSi_2$ formation. The magnetic perpendicular Au/Co interface anisotropy K_{1s} on

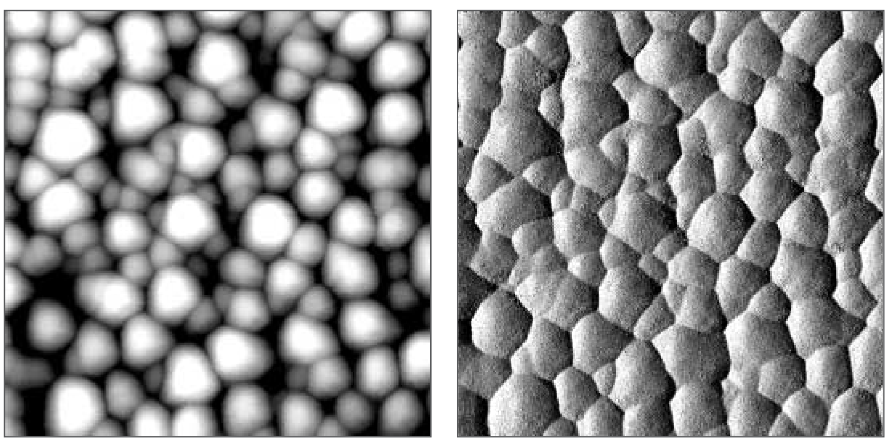

a **b**

FIGURE 1 Scanning tunneling micrograph $100 \times 100\ nm^2$ of Au/10 ML Cu/4 ML grown at 200 °C deposited on a Si (111) substrate 2° off toward the $[\bar{1}\bar{1}2]$ direction: **a** topographic image, **b** current image

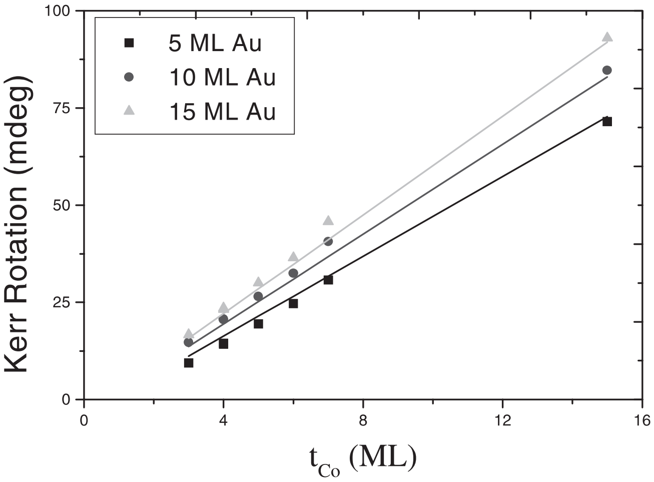

FIGURE 2 Saturated polar Kerr rotation as a function of Co thickness for an Au/Co/Au multilayer deposited on 4 ML Cu grown at 200 °C

the contrary was found to be strongly dependent on the Cu deposition temperature and only slightly dependent on Au buffer thickness: $K_{1s} = 0.5\,\mathrm{J/m^2}$ for 100 °C Cu deposition temperature and $K_{1s} = 0.3\,\mathrm{J/m^2}$ for 200 °C. For higher Co thicknesses t_{Co} ($t_{Co} > 7$ ML for 2 ML Cu deposited at 100 °C and $t_{Co} > 4$ ML for 4 ML Cu deposited at 200 °C), the easy magnetization axis lies in the film plane. In this case, a uniaxial magnetic anisotropy was observed with the easy magnetization axis parallel to the monoatomic steps of the vicinal surface. As expected, this uniaxial in-plane magnetic anisotropy (Fig. 3) increases with the atomic step density and then with the miscut angle of the vicinal surface [13].

Before investigating the crystallographic and magnetic properties of Au/Co/Au/Cu thin films using SHG measurements, we first study the influence of structural imperfections at the SiO_2/Si interface induced by substrate misorientation. Azimuthal SHG (A-SHG) analysis has been successfully performed to reveal the symmetry characteristics of the vicinal Si (111) surface (Fig. 4). This surface exhibits a C_{1v} symmetry superimposed onto the classical threefold symmetry due to (111) interface contribution [14]. The basic idea of the experimental data fit procedure is to consider the symmetry of the surface arrangement and to split the respective tensor into contributions representing the various symmetry axes. The second harmonic response of a surface layer can be written in the dipole approximation as

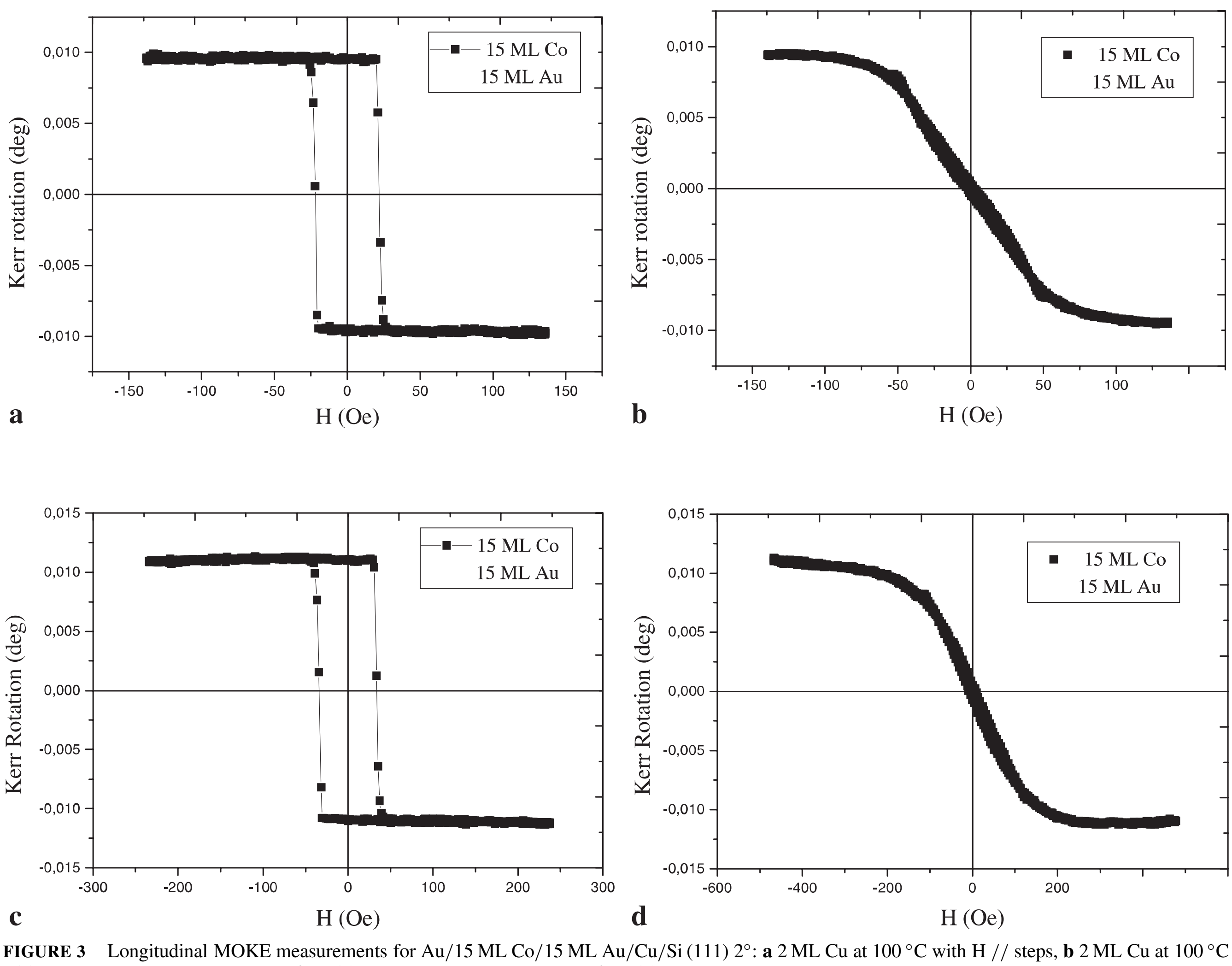

FIGURE 3 Longitudinal MOKE measurements for Au/15 ML Co/15 ML Au/Cu/Si (111) 2°: **a** 2 ML Cu at 100 °C with H // steps, **b** 2 ML Cu at 100 °C with H perp. steps, **c** 4 ML Cu at 200 °C with H // steps, **d** 4 ML Cu at 200 °C with H perp. steps

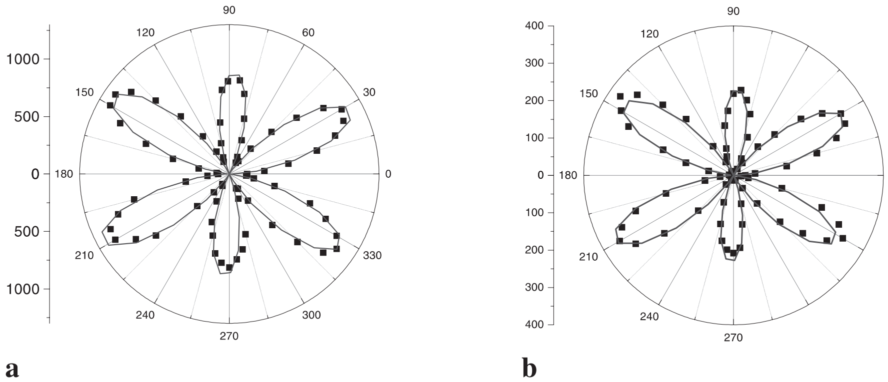

FIGURE 4 A-SHG measurements for s-polarized SH intensity for p-polarized illumination on a Si/SiO_2 interface. **a** 2° off, **b** 6° off

in [15]:

$$P_i(2\omega) = \chi_{ijk} : E_j(\omega)E_k(\omega) \quad (1)$$

where i, j, k denote vector components with respect to the x, y, z coordinate system and the sum convention rule applies. χ_{ijk} reflects the surface symmetry and is the third-rank susceptibility tensor. For a vicinal (111) surface, the azimuthal non-linear reflectivity versus the rotation angle Φ is well described using the simple phenomenological laws for each polarization configuration [16]:

$$\begin{aligned} S_{in}-S_{out} &: I = |A \sin 3\Phi + B \sin \Phi|^2 \\ P_{in}-S_{out} &: I = |A \sin 3\Phi + B \sin \Phi + C \sin 2\Phi|^2 \\ S_{in}-P_{out} &: I = |A \sin 3\Phi + B \sin \Phi + C \sin 2\Phi + D|^2 \\ P_{in}-P_{out} &: I = |A \sin 3\Phi + B \sin \Phi + C \sin 2\Phi + D|^2 \end{aligned} \quad (2)$$

The values of A, B, C and D are determined by fitting the experimental data with the above laws using a least square fit procedure. In these expressions, we must take into account the multiple reflections at each interface; however, as we will see below, the A-SHG experiments reflect mostly the structural symmetry of the upper interface.

In order to check the propagation of the vicinal character of Si substrate through the metallic multilayer, we have studied the evolution of the A-SH signal as a function of Au thickness in Au/Cu/Si (111) 2° off structures for all polarization configurations. A typical A-SHG measurement in the $S_{in}-S_{out}$ configuration is shown in Fig. 5a. A uniaxial symmetry contribution is clearly seen in the angular dependence of the azimuthal reflectivity signal. The phenomenological law $I = |A \sin 3\Phi + B \sin \Phi|^2$ describes the SH reflectivity very well; the values of A and B, determined by fitting the experimental data with the above law, increase with Au thickness. When t_{Au} increases, the electromagnetic field amplitude of the fundamental light slightly decreases on the Au/Cu and Cu/Si interfaces, inducing a reduction of their contribution to the total A-SHG signal. The contribution of the upper interface air/Au thus becomes predominant and the azimuthal reflectivity comes essentially from the structural symmetry of the surface. The ratio B/A of the uniaxial component versus the threefold symmetry, which is a clear signature of the vicinal character, does not depend on the Au thickness (Fig. 5b). This behavior implies that the step structure of the Si (111) surface is macroscopically duplicated up to a rather thick Au thickness (at least $t_{Au} = 20$ ML).

A similar analysis has been performed for the $P_{in}-S_{out}$ polarization configuration, for which the A-SHG intensity can be described using the phenomenological law corresponding to this specific configuration: $I = |A \sin 3\Phi + B \sin \Phi + C \sin 2\Phi|^2$. We observe an increase of the different SHG intensity contributions (A, B, C) with Au thickness while keeping constant the B/A and C/A ratios (Fig. 5c).

After the study of the Au/Cu buffer layer, we have carried out azimuthal experiments on the whole magnetic multilayer Au/Co/Au/Cu/Si (111). Figure 6a and b shows the s- and p-polarized SH intensity for p-polarized illumination meas-

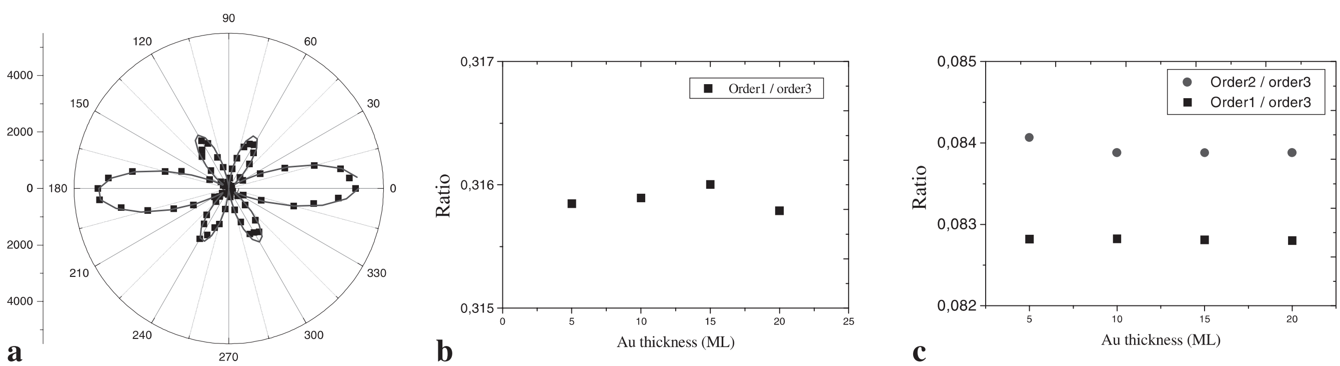

FIGURE 5 **a** Dependence of the SH reflectivity on the azimuthal angle for $S_{in}-S_{out}$ polarization. **b** Ratio between uniaxial and threefold symmetry components of the azimuthal SH reflectivity versus Au buffer thickness for A-SHG measurements for $S_{in}-S_{out}$ polarization. **c** Ratio between uniaxial and threefold symmetry components of the azimuthal SH reflectivity versus Au buffer thickness for A-SHG measurements for $P_{in}-S_{out}$ polarization

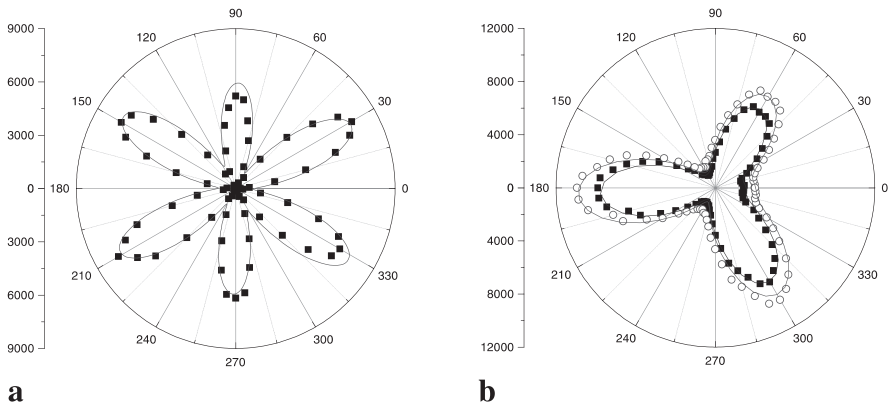

FIGURE 6 A-SHG measurements for s-polarized SH intensity for s- (**a**) and p- (**b**) polarized illumination on Au/15 ML Co/15 ML Au/2 ML Cu/Si (111) 2° off

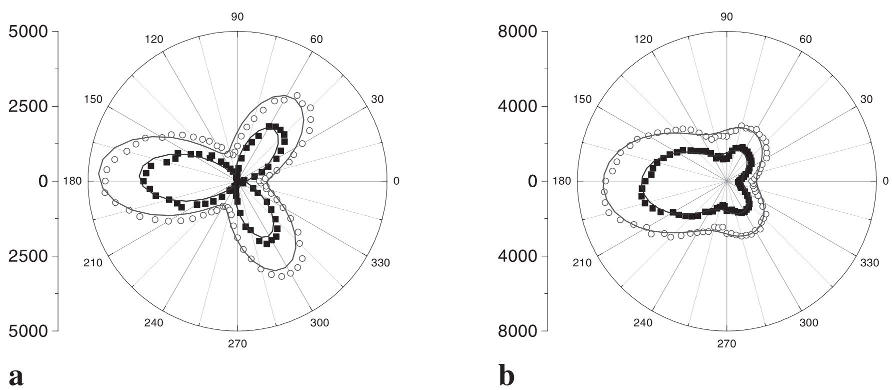

FIGURE 7 A-SHG measurements on Au/15 ML Co/15 ML Au/Cu/Si (111) 6° for: **a** 2 ML Cu grown at 100 °C, **b** 4 ML Cu grown at 200 °C

ured while the sample was rotated, for Au/15 ML Co/15 ML Au/2 ML Cu (100 °C)/Si (111) 2°. For the azimuthal measurements, we have applied a sufficient in-plane magnetic field (500 Oe) in transverse magneto-optical configuration, in order to saturate the magnetization in one direction and then in the opposite one. Using this standard technique for MO-SHG experiments, one can separate the crystallographic and magnetic contributions of the non-linear tensor elements. For the $P_{in}-S_{out}$ polarization configuration, the azimuthal SHG signal exhibits six lobes in agreement with C_{3v} symmetry, however the different peaks do not present the same magnitude, which indicates that the step structure does not preserve the (1−10) mirror plane. This configuration shows only a crystallographic contribution, as is expected for the s-polarized SH intensity in the transverse configuration. For the $P_{in}-P_{out}$ configuration, the A-SHG signal combines both crystallographic and magnetic contributions, but it shows only three main lobes and not six as observed in S_{out} signals. This difference has been explained by the presence of an isotropic term in the expression of the SH intensity for p-polarized out-coming light. The A-SHG measured in these two configurations agrees with the theoretical prediction; it also reveals the uniaxial character of the multilayer. As expected, this uniaxial symmetry is stronger in the multilayer deposited on Si 6° off.

In order to observe the influence of the copper deposition conditions on the interface roughness, SHG experiments were carried out on Au/15 ML Co/15 ML Au/Cu/Si (111) 6° for 2 ML Cu grown at 100 °C and 4 ML at 200 °C. Figure 7 clearly shows that the uniaxial character is stronger in the multilayer deposited on 4 ML at Cu (200 °C), as well as the in-plane magnetic anisotropy which favors easy magnetization along the step direction. This result is in good agreement with the longitudinal MOKE experiments.

4 Conclusion

We have investigated the non-linear optical and magneto-optical properties of Au/Co/Au/Cu multilayers deposited on vicinal Si (111) substrates, with changing film thickness, growth conditions and misorientation angle of the vicinal surface. The SHG azimuthal anisotropic reflectivity and the magnetic properties of Au/Co/Au multilayers depend strongly on both substrate misorientation and copper growth conditions. The uniaxial SHG azimuthal anisotropy is rather independent of the Au buffer thickness in the Au thickness range from 3 to 20 ML. On the contrary, it strongly depends on the Cu deposition temperature. The in-plane magnetic anisotropy shows a clear dependence on the misorientation angle of the vicinal Si (111) substrate and the easy magnetization axis is parallel to the monoatomic steps of the silicon substrate. This experiment clearly shows the powerful character of SHG azimuthal experiments since in situ STM experiments on the metallic multilayer are not able to clearly exhibit the uniaxial character of the metallic multilayer.

REFERENCES

1 N.C. Koon: Phys. Rev. Lett. **78**, 4865 (1997)
2 J. Chen, J.L. Erskine: Phys. Rev. Lett. **68**, 1212 (1992)
3 D.S. Chuang, C.A. Ballentine, R.C. O'Handley: Phys. Rev. B **49**, 15 084 (1994)
4 J.A.C. Bland, S. Hope, B. Choi, P. Bode: J. Appl. Phys. **85**, 4613 (1999)

5 R.K. Kawakami, E.J. Escorcia-Aparicio, Z.Q. Qiu: Phys. Rev. Lett. **77**, 2570 (1996)
6 G. Spierings, V. Koustos, H.A. Wieranga, D. Abraham, Th. Rasing: Surf. Sci. **287**, 749 (1993)
7 J. Wei, X.-S. Wang, J.L. Goldberg, N.C. Bartelt, E.D. Williams: Phys. Rev. Lett. **68**, 3885 (1992)
8 H. Hibino, T. Ogino: Phys. Rev. Lett. **72**, 657 (1994)
9 J. Tershoff, Y.H. Phang, Z. Zhang, M.G. Lagally: Phys. Rev. Lett. **75**, 2730 (1995)
10 S. Gallego, J. Avila, M. Martin, X. Blasé, A. Taleb, P. Dumas, M.C. Ascensio: Phys. Rev. B **61**, 12 628 (2000)
11 S. Visnovsky, R. Lopusnik, M. Nyvlt, V. Prosser, J. Ferré, C. Train, P. Beauvillain, D. Renard, R. Krishnan, J.A.C. Bland: Czech. J. Phys. **50**, 857 (2000)
12 J. Harmle, M. Nyvlt, S. Visnovsky, R. Urban, P. Beauvillain, R. Mégy, J. Ferré, L. Polerecky, D. Renard: Phys. Rev. B **64**, 155 405 (2001)
13 R.K. Kawakami, E. Escorcia-Aparicio, Z. Qiu: Phys. Rev. Lett. **77**, 2570 (1996)
14 M.A. Verheijen, C.W. Van Hasselt, T. Rasing: Surf. Sci. **251**, 467 (1991)
15 Y.R. Shen: The Principles of Nonlinear Optics (Wiley, New York 1984)
16 G. Lüpke, G. Marowsky, R. Steinhoff, A. Friedrich, B. Pettinger, D.M. Kolb: Phys. Rev. B **41**, 6913 (1990)